CENOZOIC CLIMATE – OXYGEN ISOTOPE EVIDENCE

J. D. Wright, Rutgers University, Piscataway, NJ, USA.

doi:10.1006/rwos.2001.0252

Discoveries of fossil remains of 50 million year old alligators on Ellesmere Island and 30–40 million year-old forests on Antarctica contrast sharply with our present vision of polar climates. These are not isolated discoveries or quirks of nature. An ever-growing body of faunal, floral, and geochemical evidence shows that the first half of the Cenozoic Era was much warmer than the present time. What maintained such a warm climate and could it be an analog for future global warming? To address these and other questions, one needs more than a qualitative estimate of planetary temperatures. Quantitative temperature estimates (both magnitudes and rates of change) are required to depict how the Earth's climate has changed through time. One of the most powerful tools used to reconstruct past climates during the Cenozoic (the last 65 million years of Earth's history) is the analysis of oxygen isotopes in the fossil shells of marine organisms. The calcium carbonate shells of the protist foraminifera are the most often analyzed organisms because the different species are distributed throughout surface (plank-tonic) and deep (benthic) marine environments.

Oxygen Isotope Systematics

The stable isotopes of oxygen used in paleoceanographic reconstructions are ^{16}O and ^{18}O. There are about 500 ^{16}O atoms for every ^{18}O atom in the ocean/atmosphere environment. During the 1940s, Harold Urey at the University of Chicago predicted that the $^{18}O/^{16}O$ ratio in calcite ($CaCO_3$) should vary as a function of the temperature at which the mineral precipitated. His prediction spurred on experiments by himself and others at the University of Chicago who measured $^{18}O/^{16}O$ ratios in $CaCO_3$ precipitated in a wide range of temperatures, leading to the use of stable oxygen isotope measurements as a paleothermometer.

To determine oxygen isotopic ratios, unknown $^{18}O/^{16}O$ ratios are compared to the known $^{18}O/^{16}O$ ratio of a standard. The resulting values are expressed in delta notation, $\delta^{18}O$, where:

$$\delta^{18}O = \frac{^{18}O/^{16}O_{sample} - {}^{18}O/^{16}O_{standard}}{^{18}O/^{16}O_{standard}} \times 1000 \quad [1]$$

Carbonate samples are reacted in phosphoric acid to produce CO_2. To analyze water samples, CO_2 gas is equilibrated with water samples at a constant temperature. Given time, the CO_2 will isotopically equilibriate with the water. For both the carbonate and water samples, the isotopic composition of CO_2 gas is compared with CO_2 gas of known isotopic composition. There are two standards for reporting $\delta^{18}O$ values. For carbonate samples, the reference standard is PDB, which was a crushed belemnite shell (*Belemnitella americana*) from the Peedee formation of Cretaceous age in South Carolina. The original PDB material has been exhausted, but other standards have been calibrated to PDB and are used as an intermediate reference standard through which a PDB value can be calculated. For measuring the isotopic composition of water samples, Standard Mean Ocean Water (SMOW) is used as the reference. The SMOW reference was developed so that its $\delta^{18}O_{water}$ value is 0.0‰ (parts per thousand) and approximates the average oxygen isotopic composition of the whole ocean. Deep ocean $\delta^{18}O_{water}$ values are close to the SMOW value, ranging from -0.2 to 0.2‰. In contrast, surface ocean $\delta^{18}O_{water}$ values exhibit a much greater variability, varying between -0.5 and $+1.5$‰.

Oxygen Isotope Paleothermometry

Early studies into the natural variations in oxygen isotopes led to the development of a paleotemperature equation. The temperature during the precipitation of calcite can be estimated by measuring the $\delta^{18}O$ value in calcite-secreting organisms (foraminifera, corals, and mollusks) and the value of the water in which the organisms live. The various paleotemperature equations all follow the original proposed by Sam Epstein and his colleagues (University of Chicago):

$$T = 16.5 - 4.3 \times (\delta^{18}O_{calcite} - \delta^{18}O_{water}) + 0.14 \times (\delta^{18}O_{calcite} - \delta^{18}O_{water})^2 \quad [2]$$

where T and $\delta^{18}O_{water}$ are the temperature (°C) and oxygen isotope value of the water in which the

organism lived[1], and $\delta^{18}O_{calcite}$ is the oxygen isotope value of calcite measured in the mass spectrometer.

Eqn [2] shows that the changes in $\delta^{18}O_{calcite}$ are a function of the water temperature and $\delta^{18}O_{water}$ value. A one-to-one relationship between $\delta^{18}O_{calcite}$ and $\delta^{18}O_{water}$ values dictates that a change in the $\delta^{18}O_{water}$ term will cause a similar change in the measured $\delta^{18}O_{calcite}$ value. However, an inverse relationship between $\delta^{18}O_{calcite}$ and T changes dictates that for every 1°C increase in temperature, there is a 0.23‰ decrease in the measured $\delta^{18}O_{calcite}$ value. These relationships enable us to interpret $\delta^{18}O_{calcite}$ changes generated from foraminifera, corals, and mollusks. For many years, the convention was to plot $\delta^{18}O_{calcite}$ values with the axis reversed (higher values to the left or bottom) so that $\delta^{18}O$ records reflect climate changes (e.g., colder to the left or bottom). More recently, there has been a trend among some scientists to plot $\delta^{18}O_{calcite}$ values without reversing the axis.

The paleotemperature equation contains two unknowns (temperature, $\delta^{18}O_{water}$). Although temperature is the main target in reconstructions, one cannot ignore the $\delta^{18}O_{water}$ term. In the modern ocean, the equator-to-pole gradient measured in planktonic foraminifera $\delta^{18}O_{calcite}$ values is ~ 5.0‰ and largely reflects the temperature gradient (~ 28°C). However, if temperature were the sole influence on modern $\delta^{18}O_{calcite}$ values, the equator-to-pole gradient would be ~ 6.5‰ (28°C × 0.23‰/°C). The attenuated $\delta^{18}O_{calcite}$ gradient measured in planktonic foraminifera reflects the surface ocean $\delta^{18}O_{water}$ variability. Therefore, a key to using $\delta^{18}O_{calcite}$ records as indicators of past climates is to understand the hydrographic parameters that produce the modern $\delta^{18}O_{calcite}$ gradient. For instance, ignoring the $\delta^{18}O_{water}$ term results in a 5–6°C underestimation compared to the observed temperature gradient. This occurs largely because tropical temperature estimates will be too cold (~ 4°C) whereas polar estimates will be warm (~ 1–2°C).

$\delta^{18}O$ Variation in the Natural Environment

$\delta^{18}O_{water}$ values in the ocean/atmosphere system vary both spatially and temporally because fractionation between the $H_2{}^{18}O$ and $H_2{}^{16}O$ molecules is temperature-dependent in the hydrologic cycle and follows the Rayleigh Distillation model (**Figure 1**). In general, water vapor evaporates at low latitudes and precipitates at higher latitudes. Fractionation during evaporation concentrates the lighter $H_2{}^{16}O$ molecule in the water vapor, leaving the water enriched in $H_2{}^{18}O$. On average, the $\delta^{18}O_{water}$ value of water vapor is 9‰ lower than its source water (**Figure 1**). Fractionation during condensation concentrates the $H_2{}^{18}O$ molecules in the precipitation (rain/snow) by ~ 9‰. Therefore, if all of the water evaporated in the tropics rained back into the tropical oceans, there would be no net change in the $\delta^{18}O_{water}$ term. However, some water vapor is transported to higher latitudes. If the clouds remain a closed system (i.e., mid-to-high latitude evaporation does not influence the $\delta^{18}O_{water}$ value in the clouds[2]), then precipitation will further deplete the clouds (water vapor) in $H_2{}^{18}O$ relative to $H_2{}^{16}O$. Consequently, the $\delta^{18}O$ value of water vapor decreases from the original value as water vapor condenses into precipitation (**Figure 1**) and the cloud that formed from the evaporation in the tropics will

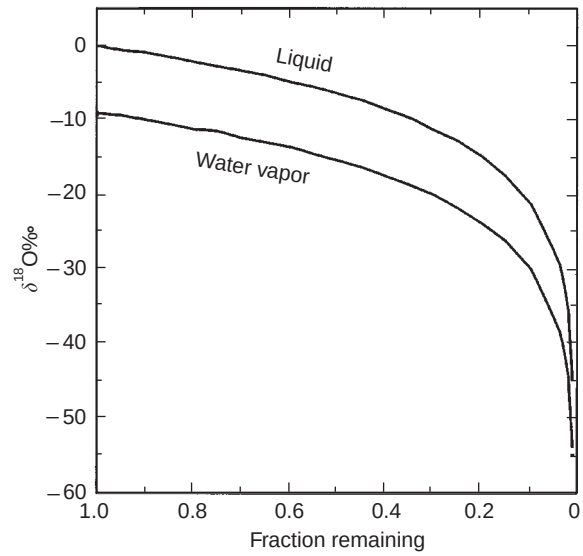

Figure 1 Rayleigh distillation model showing the effects of evaporation and precipitation on the $\delta^{18}O$ values in the vapor and liquid phases. The initial conditions are a temperature of 25°C and $\delta^{18}O_{water}$ value of 0‰. This model also assumes that it is a closed system, meaning that water vapor is not added once the cloud moves away from the source regions. As clouds lose moisture, fractionation during the condensation further lowers the $\delta^{18}O_{water}$ value in the water vapor.

[1] $\delta^{18}O$ calcareous deposits are commonly reported relative to a carbonate standard, PDB (Peedee belemnite), and not SMOW (Standard Mean Ocean Water). PDB is 22‰ relative to SMOW.

[2] Many island or coastal regions have significantly higher $\delta^{18}O_{water}$ values relative to continental locations at similar latitudes. This occurs because local evaporation increases the $\delta^{18}O_{water}$ values, thus resetting the initial conditions for Rayleigh distillation to occur.

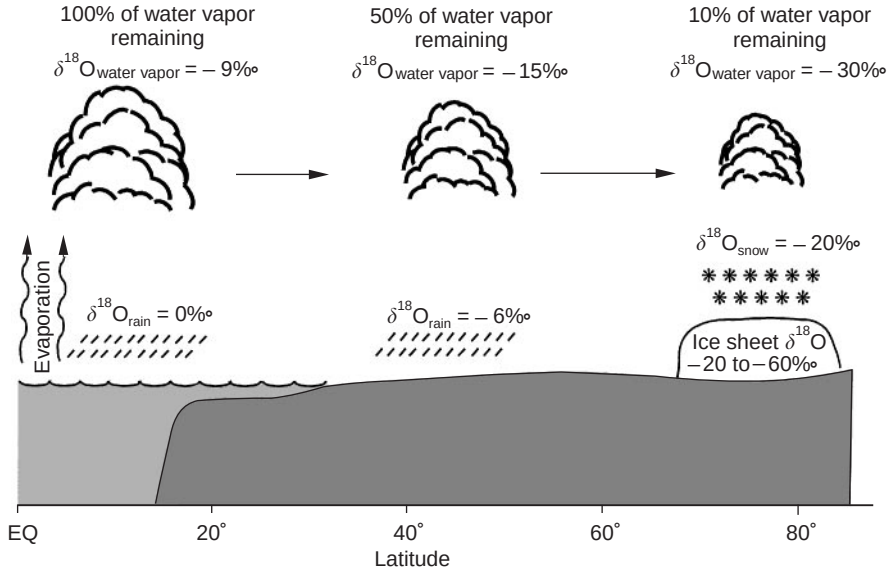

Figure 2 Illustration of the Rayleigh distillation process on $\delta^{18}O$ values as clouds move over land and into the polar regions. Decreasing air temperatures cause moisture to rain/snow out of the cloud. Fractionation of the oxygen isotopes during condensation further decreases values. By the point that a cloud reaches the high latitudes, less than 10% of the original water vapor remains. Snowfall on Antarctica has values between -20 and $-60‰$. The average $\delta^{18}O$ value for ice on Antarctica is $\sim -40‰$.

eventually lose moisture, fractionating the $\delta^{18}O_{water}$ value of the remaining water vapor (**Figures 1** and **2**). By the time 50% of the initial moisture precipitates, the $\delta^{18}O$ value of the water vapor will be $\sim -15\%$, while precipitation will be $\sim -6‰$. Once the cloud reaches the poles, over 90% of the initial water vapor will have been lost, producing $\delta^{18}O$ values of snow less than $-20‰$. Snow at the South Pole approaches $-60‰$. There is a strong relationship between $\delta^{18}O$ values in precipitation and air mass temperatures because air temperature dictates how much water vapor it can hold, and the $\delta^{18}O$ values of the precipitation is a function of the amount of water remaining in the clouds (**Figure 3**).

Spatial Variations in $\delta^{18}O_{water}$ of Modern Sea Water

The evaporation/precipitation process that determines the $\delta^{18}O_{water}$ values of precipitation (e.g.,

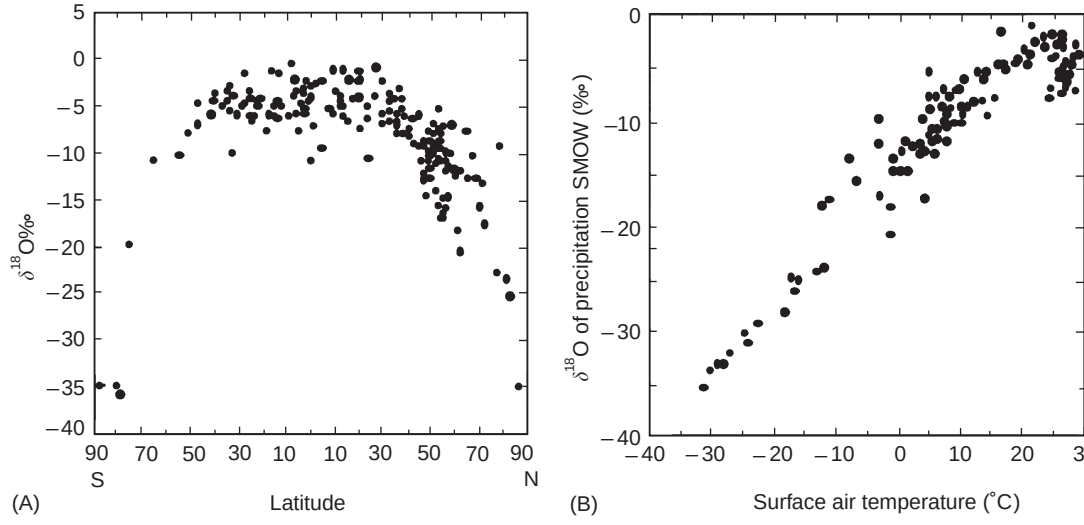

Figure 3 Mean annual $\delta^{18}O$ water of precipitation (rain/snow) versus mean annual temperatures. The correlation between $\delta^{18}O$ values and latitude (A) is a function of temperature (B). The rainout/fraction of water remaining, and hence the fraction of $\delta^{18}O$ values, is determined by the cloud temperatures. Latitude is the dominant effect shown here. The scatter among sites at similar latitude results from elevation differences as well as differences in the distance from the ocean.

Figure 1) also controls the $\delta^{18}O_{water}$ values in regions in the ocean. At any one time, the volume of water being transported through the hydrologic cycle (e.g., atmosphere, lakes, rivers, and groundwater) is small compared to the volume of water in the oceans (1:130). Therefore, the hydrologic cycle can influence the whole ocean $\delta^{18}O_{water}$ value only by creating a new or enlarging an existing reservoir (e.g., glacier/ice sheets). In contrast, evaporation/precipitation processes will change the $\delta^{18}O_{water}$ and salinity values in the surface waters because only the thin surface layer of the ocean communicates with the atmosphere. As noted above, the process of evaporation enriches surface water in $H_2{}^{18}O$ molecules and salt because the water vapor is enriched in $H_2{}^{16}O$ molecules. For this reason, high salinity sea water has a high $\delta^{18}O_{water}$ value and vice versa. More specifically, tropical and subtropical surface water $\delta^{18}O_{water}$ values are $\sim 1‰$ higher than mean ocean water values (**Figure 4**). Interestingly, subtropical $\delta^{18}O_{water}$ values are higher than tropical values even though evaporation is higher in the tropics. Atmospheric circulation patterns produce intense rainfall in the tropics to offset some of the evaporation, whereas very little rain falls in the subtropical regions. Because evaporation minus precipitation (E − P) is greater in the subtropics, these regions have higher salinity and $\delta^{18}O_{water}$ values. In contrast, subpolar and polar regions have greater precipitation than evaporation; hence, high-latitude surface waters have low salinity and $\delta^{18}O_{water}$ values that approach $-0.5‰$ (**Figure 4**).

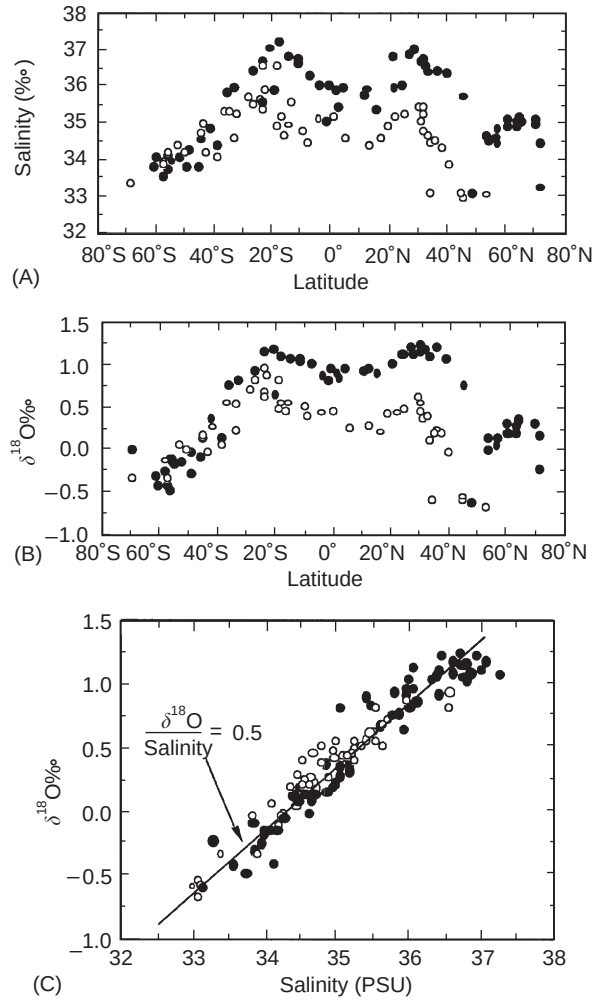

Figure 4 The salinity (A) and $\delta^{18}O_{water}$ values (B) measured in the open Atlantic (●) and Pacific (○) oceans. Note the higher values in the tropical and subtropical region relative to the subpolar and polar regions. Evaporation and precipitation/runoff processes produce similar patterns in salinity and $\delta^{18}O_{water}$ values which is illustrated by the linearity in the $\delta^{18}O$ versus salinity plot (C). The ocean-to-ocean difference between the Atlantic and Pacific results from a net transfer of fresh water from the Atlantic to the Pacific.

Temporal Variations

Variations in the amount of water stored on land through time, usually in the form of ice, can have a significant effect on the mean ocean $\delta^{18}O_{water}$ value, and hence, the marine $\delta^{18}O_{calcite}$ record. At present, high-latitude precipitation returns to the oceans through summer ice/snow melting. During glacial periods, snow and ice accumulate into large ice sheets. Because the difference in ice sheet and mean ocean values is large ($\delta^{18}O_{ice} = -35$ to $-40‰$ vs. $\delta^{18}O_{water}$ mean ocean $= \sim 0‰$), ice sheet fluctuations are reflected in mean oceanic $\delta^{18}O_{water}$ values. This relationship can be illustrated by examining how the mean ocean $\delta^{18}O_{water}$ value increased during the last glacial maximum (LGM) relative to the present (**Figure 5**). During the LGM, water stored in continental ice lowered global sea level by 120 m, removing $\sim 3\%$ of the ocean's volume. Thus, the mean ocean $\delta^{18}O_{water}$ value increased by $1.2‰$ during the LGM relative to the present (**Figure 5**).

Pleistocene Oxygen Isotope Variations

The first systematic downcore examination of the marine stable isotope record was made by Cesaré Emiliani during the 1950 s on $\delta^{18}O_{calcite}$ records generated from planktonic foraminifera in Caribbean deep-sea cores. Emiliani recognized the cyclic pattern of low and high $\delta^{18}O_{calcite}$ values and concluded that these represented glacial–interglacial intervals. Emiliani identified the seven most recent climate cycles and estimated that they spanned the last 280 000 years. (Current age estimates indicate that the duration of the cycles is approximately 525 000

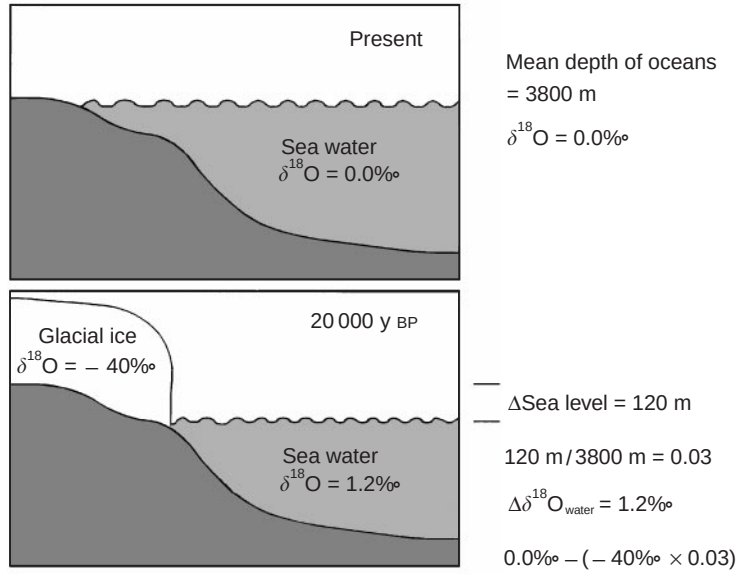

Figure 5 The effect of building or removing large ice sheets on the $\delta^{18}O$ composition of the ocean can be significant. The removal of 3% of the ocean's water during the last glacial maximum lowered sea level by 120 m. The $\delta^{18}O$ difference between the ocean and the ice is 40‰, causing a whole ocean $\delta^{18}O$ change of 1.2‰. The reverse process occurs during the melting of large ice sheets. If the Antarctic and Greenland ice were to melt, then sea level would rise $\sim$70 m. The volume of water stored in these ice sheets is equivalent to $\sim$2% of the water in the ocean. Therefore, the mean $\delta^{18}O$ value of the ocean would decrease by 0.7–0.8‰ (relative to PDB).

years.) To apply the paleotemperature equation to these records, Emiliani estimated that ice sheet-induced ocean $\delta^{18}O_{water}$ variability was relatively small, 0.3‰. (As shown above, the maximum glacial–interglacial ice sheet signal was closer to 1.2‰.) Therefore, most of the $\delta^{18}O_{calcite}$ variability between glacial and interglacial intervals represented temperature changes of 5–10°C. Emiliani divided the $\delta^{18}O_{calcite}$ record into warm stages (designated with odd numbers counting down from the Holocene) and cold stages (even numbers). Hence, 'Isotope Stage 1' refers to the present interglacial interval and 'Isotope Stage 2' refers to the LGM (**Figure 6**). During the 1960 s and 1970s, many argued that most of the glacial to interglacial difference in $\delta^{18}O_{calcite}$ values resulted from ice volume changes. Nicholas Shackleton of Cambridge University made the key observation that benthic foraminiferal $\delta^{18}O$ values show a glacial to interglacial difference of $\sim$1.8‰. If the ice volume contribution was only 0.3‰ as argued by Emiliani, then the deep ocean temperatures would have been 6–7°C colder than the present temperatures of 0–3°C. Sea water freezes at -1.8°C, precluding Emiliani's 'low' ice volume estimate. By the early 1970s, numerous $\delta^{18}O$ records had been generated and showed a cyclic variation through the Pleistocene and into the late Pliocene. One hundred oxygen isotope stages, representing 50 glacial–interglacial cycles, have been identified for the interval since 2.6 million years ago (Ma) (**Figure 6**).

Cenozoic $\delta^{18}O$ Records

The first Cenozoic $\delta^{18}O$ syntheses based on foraminiferal $\delta^{18}O$ records were produced during the mid-1970 s. Nicholas Shackleton and James Kennett produced a composite benthic $\delta^{18}O$ record for the Cenozoic from cores to the south of Australia. A second group led by Samuel Savin generated low-latitude planktonic and benthic foraminiferal $\delta^{18}O$ syntheses. Both records are important to understanding Cenozoic climate changes. Benthic foraminiferal records best reflect global temperature and ice volume changes. Additional advantages of the benthic foraminiferal composite include: (1) deep-ocean temperatures are more uniform with respect to horizontal and vertical gradients; (2) deep-ocean $\delta^{18}O_{water}$ values are less variable compared to the large surface water changes; (3) the deep ocean approximates high-latitude surface water conditions where deep waters originated during the Cenozoic (i.e., Antarctica, northern North Atlantic); and (4) many benthic foraminifera taxa are long-lived so that one species can be used to construct records spanning several millions of years in contrast to planktonic taxa which have shorter

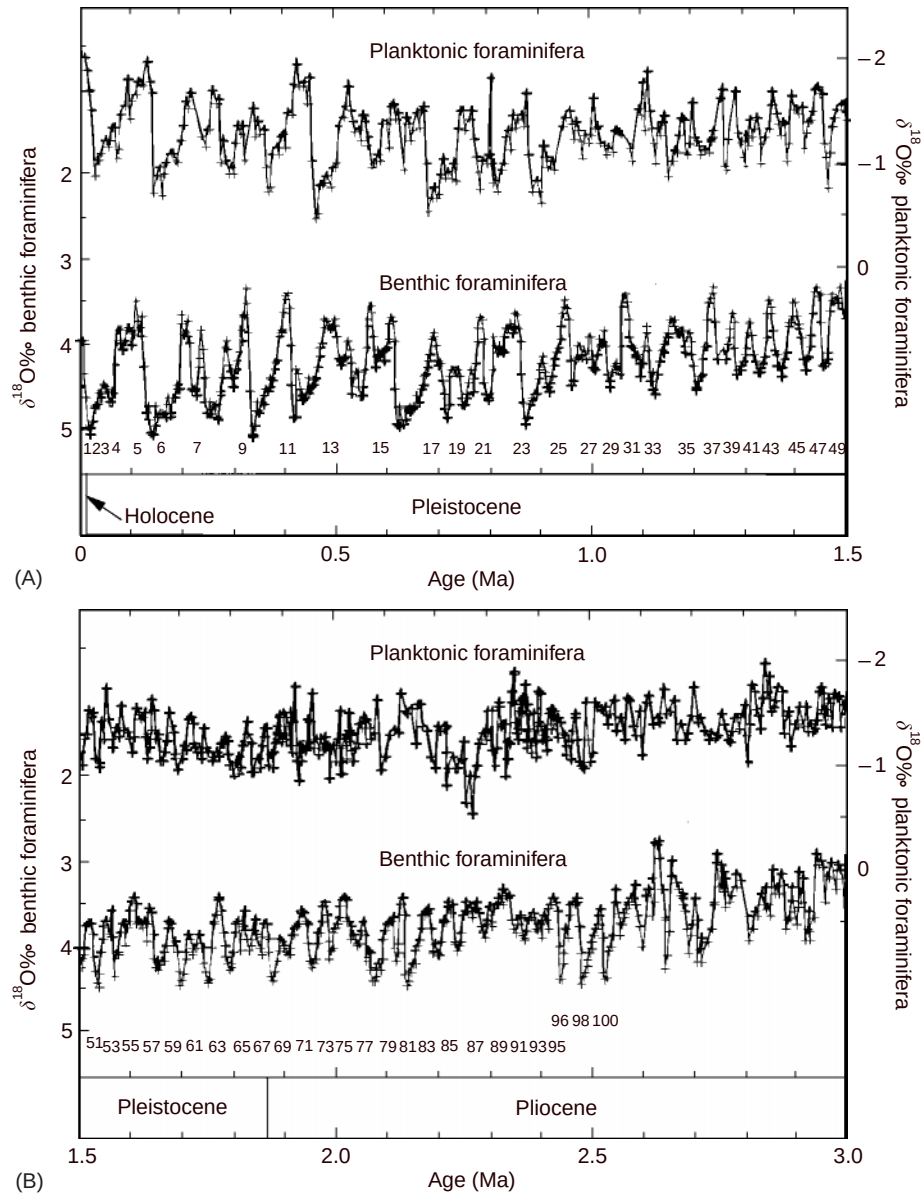

Figure 6 Planktonic and benthic foraminiferal $\delta^{18}O$ records for the last 3 million years. Note the high frequency signals in the records. For the interval between 3 and 1 Ma, a 40 000 year cycle dominates the records. After 1 Ma, the beat changes to a 100 000 year cycle and the amplitudes increase (relative to PDB).

durations and require records to be spliced together from several species.

Low-latitude planktonic foraminiferal $\delta^{18}O$ records are good proxies for tropical sea surface temperatures. Tropical temperatures are an important component of the climate system because they influence evaporation, and hence, total moisture in the atmosphere. Planktonic and benthic foraminiferal $\delta^{18}O$ comparison allows one to assess equator-to-pole as well as vertical temperature gradients during the Cenozoic, and thus, to determine planetary temperature changes. Finally, much of the climatic change in the last 65 million years has been ascribed to poleward heat transport or greenhouse gas fluctuations. General circulation models indicate that each mechanism should produce different temperature patterns that can be approximated with the planktonic and benthic $\delta^{18}O$ records.

The first benthic $\delta^{18}O$ syntheses generated, as well as more recent compilations, show the same long-term patterns. After the Cretaceous–Tertiary (K/T) boundary events, deep-water $\delta^{18}O$ values remained relatively constant for the first 7 million years of the Paleocene (**Figure 7A**). At 58 Ma, benthic foraminiferal $\delta^{18}O$ values began a decrease over the next 6 My that culminated during the early Eocene

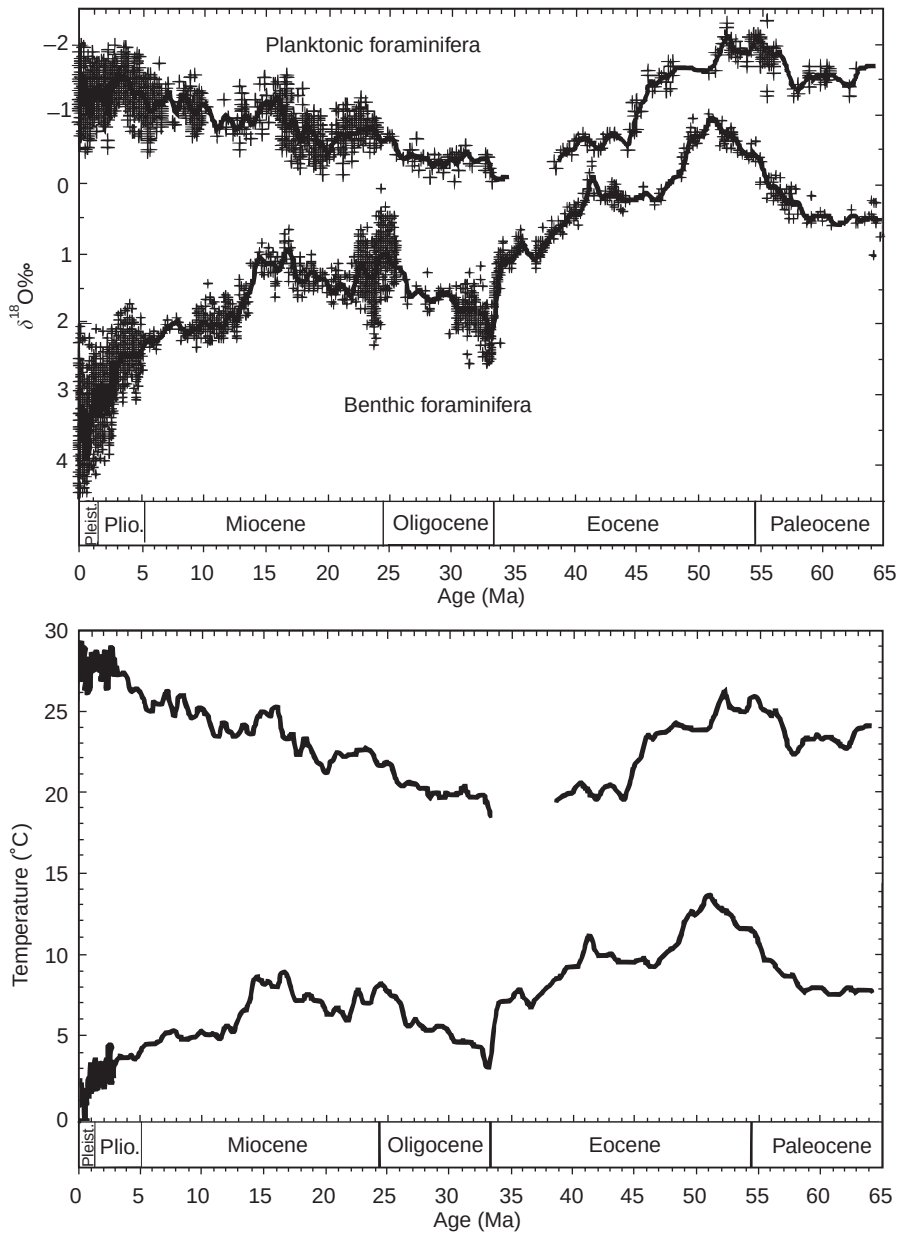

Figure 7 (A) Planktonic and benthic foraminiferal $\delta^{18}O$ composite records representing the tropical surface and deep ocean conditions (relative to PDB). The thick line through both records was generated using a 1 million year Gaussian filter. (B) Temperature estimates based on planktonic and benthic records and ice volume estimates discussed in the text.

with the lowest recorded value ($-0.5‰$) of the Cenozoic. Following this minimum at 52 Ma, $\delta^{18}O$ values increased by 5.5‰, recording maximum values ($\sim 5‰$) during the glacial intervals of Pleistocene (**Figure 6**). The first part of this long-term change was a gradual increase of 2‰ through the end of the Eocene (52–34 Ma). The remainder of the increase was accomplished through large steps at the Eocene/Oligocene boundary (~ 33.5 Ma), during the middle Miocene (ca. 15–13 Ma) and late Pliocene (ca. 3.2–2.6 Ma). After 2.6 Ma, the amplitude of the high-frequency signal increased to $> 1‰$, reaching 1.8‰ over the past 800 thousand years.

Planktonic and benthic foraminiferal $\delta^{18}O$ values co-varied in general during the early Cenozoic (6.5–34 Ma). Values averaged about $-1‰$ between 65 and 58 Ma, before decreasing to $-2.5‰$ during the early Eocene, recording the lowest values of the Cenozoic (**Figure 7A**). From 52 to 33 Ma, planktonic foraminiferal values increased by 2‰. In spite of a break in the latest Eocene record, it appears

that the tropical ocean differed from the deep ocean across the Eocene/Oligocene boundary. For much of the Oligocene ($\sim$ 33–25 Ma), planktonic foraminiferal $\delta^{18}O$ values remained unusually high, averaging $-0.5‰$. Beginning around the Oligocene/Miocene boundary ($\sim$ 25 Ma), planktonic foraminiferal $\delta^{18}O$ values began a long-term decrease, culminating in the Pleistocene with average values of $-1.5‰$. In contrast, the benthic $\delta^{18}O$ record permanently changed during the middle Miocene $\delta^{18}O$ shift and late Pliocene increase.

Apportioning the $\delta^{18}O$ changes recorded by the benthic and planktonic foraminifera between temperature and ice volume changes requires knowledge of, or reasonable estimates for, one of these parameters. One promising tool that may help discriminate between each effect is the Mg/Ca ratio measured in benthic foraminifera. Initial studies using Mg/Ca ratios confirmed the long-term temperature changes during the Cenozoic calculated using the $\delta^{18}O$ record and other climate proxies. If verified, this record implies that small ice sheets grew during the middle and late Eocene and fluctuated in size throughout the Oligocene to Miocene. At present, the Mg/Ca record lacks the resolution for key intervals and still requires verification of interspecies offsets before it can be applied unequivocally to isolate the ice volume-induced $\delta^{18}O_{water}$ component in the foraminiferal $\delta^{18}O$ records. For the discussion that follows, glacialogical evidence is used to estimate the ice volume/$\delta^{18}O_{water}$ variations.

The Greenhouse World

The oldest unequivocal evidence for ice sheets on Antarctica, ice-rafted detritus (IRD) deposited by icebergs in the ocean, places the first large ice sheet in the earliest Oligocene. Thus, it is reasonable to assume that ice sheets were small to absent and that surface and deep-water temperature changes controlled much if not all the $\delta^{18}O$ change prior to 34 Ma. The modern Antarctic and Greenland ice sheets lock up $\sim$ 2% of the total water in the world's ocean. If melted, these ice sheets would raise global sea level by $\sim$ 70–75 m and mean ocean $\delta^{18}O_{water}$ value would decrease to $-0.9‰$ PDB (see above). One can then apply eqn [2] to the benthic and planktonic foraminiferal $\delta^{18}O$ records to estimate deep- and surface-ocean temperatures for the first half of the Cenozoic (*c.* 65–34 Ma).

During the early to middle Paleocene, deep-water temperatures remained close to 10°C (**Figure 7B**). The 1‰ decrease between 58 and 52 Ma translates into a deep-water warming of 4°C, reaching a high of 14°C. This is in sharp contrast to the modern deep-water temperatures, which range between 0 and 3°C. Following the peak warmth at 52 Ma, the 2‰ increase in benthic foraminiferal values indicates that the deep waters cooled by 7°C and were 7°C by the end of the Eocene. If small ice sheets existed during the Paleocene and Eocene, then temperature estimates would be on the order of 1°C warmer than those calculated for the ice-free assumption. (Some data indicate that smaller ice sheets may have existed on the inland parts of Antarctica during the late Eocene. However, these were not large enough to deposit IRD in the ocean. Therefore, their effect on the $\delta^{18}O$ values of the ocean was probably less than 0.3‰.)

Tropical surface water temperatures warmed from 22 to 24°C, based on eqn [2], at the beginning of the Cenozoic to 28°C during the early Eocene (52 Ma; **Figure 7B**). The higher estimate is similar to temperatures in the equatorial regions of the modern oceans. Planktonic foraminiferal $\delta^{18}O$ values recorded a long-term increase of by 2‰ (-2.5 to $-0.5‰$) through the remainder of the Eocene. Just prior to the Eocene/Oligocene boundary, tropical surface water temperatures were $\sim$ 21°C, ending the long-term tropical cooling of 7°C from 52 to 34 Ma.

The Ice House World of the Last 33 Million Years

As mentioned above, southern ocean cores contain IRD at and above the Eocene/Oligocene boundary. Widely distributed IRD and glacial tills on parts of the Antarctic continental margin representing the Oligocene to Recent mark the onset of large ice sheets. Whether these sediments represent persistent or periodic ice cover is uncertain. At least some ice was present on Antarctica during the Oligocene to early Miocene. The Antarctic ice sheet has been a fixture since the middle Miocene ($\sim$ 15 Ma). Our record of Northern Hemisphere ice sheets suggests that they were small or nonexistent prior to the late Pliocene. For the purpose of estimating surface and deep temperatures, an ice volume estimate slightly lower than the modern will be applied for the interval that spans from the Oligocene into the middle Miocene (33–15 Ma). For the interval between 15 and 3 Ma, ice volumes were probably similar to those of today. From 3 Ma, ice volumes ranged between the modern and LGM. Using these broad estimates for ice volumes, mean ocean $\delta^{18}O_{water}$ values for those three intervals were -0.5, -0.22, and 0.4‰ PDB, respectively. The 0.4‰ estimate reflects the average between the maximum and minimum conditions during the Plio-Pleistocene. As

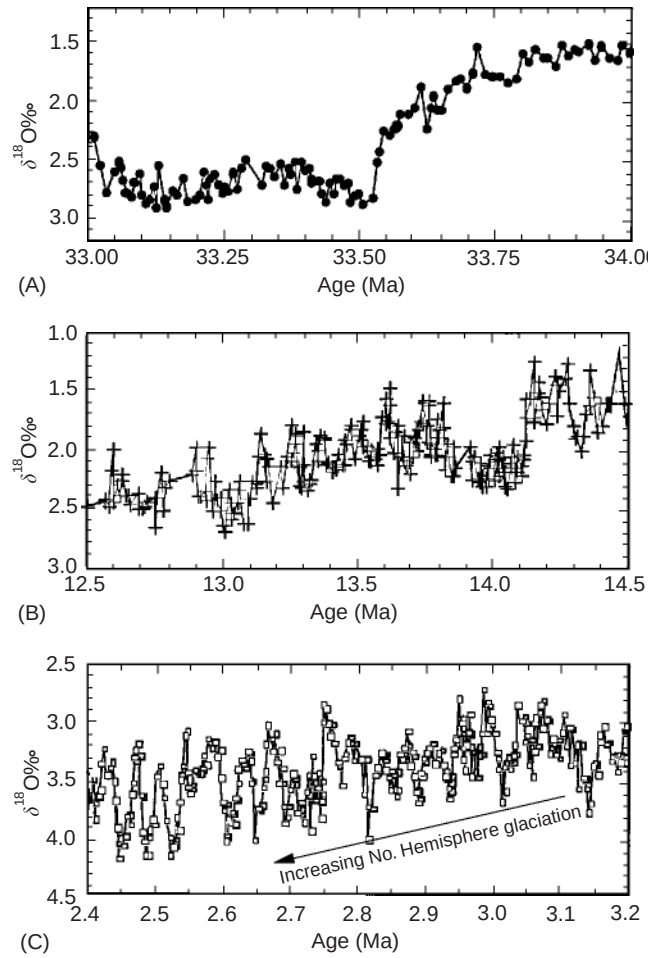

Figure 8 High-resolution δ^{18}O records representing the Eocene/Oligocene boundary (A), middle Miocene (B), and late Pliocene (C) δ^{18}O shifts (relative to PDB).

noted above, the largest portion of the high frequency signal is controlled by ice volume changes.

The benthic foraminiferal δ^{18}O increase at the Eocene/Oligocene boundary occurred rapidly ($\sim$ 10 000 years; **Figure 8A**). At the peak of the Eocene/Oligocene boundary event, benthic foraminifera recorded δ^{18}O values similar to modern values. Using the ice volume assumption from above, deep-water temperatures approached modern deep-ocean temperatures (3°C). This marks an important transition from the relatively warm oceans of the Paleocene and Eocene to the cold deep waters of the Oligocene to present. This switch to a cold ocean where bottom waters formed at near-freezing temperatures heralded the development of the psychrosphere. Following the Eocene/Oligocene boundary, deep-water temperatures began a long-term warming over the next 18 million years (33–15 Ma). The coldest deep-water temperatures of 3°C were recorded at 33 Ma, while temperatures reached 9°C at $\sim$ 25 and $\sim$ 15 Ma (**Figure 7B**).

There is a gap in the planktonic foraminiferal δ^{18}O record for the latest Eocene that hampers our assessment of tropical response during Eocene/Oligocene climate event. However, it is clear from the data that do exist that the planktonic response across the Eocene/Oligocene boundary differed from the benthic response. The planktonic foraminiferal δ^{18}O values for the early Oligocene are similar to late Eocene values, whereas the benthic values recorded a 1.5‰ increase. Planktonic foraminiferal records from other regions that span the Eocene/Oligocene boundary indicate that the surface water δ^{18}O increase was on the order of 0.5‰. This change is approximately equal to the effect of the modern Antarctic ice sheet. Combined with the physical evidence, it seems probable that the planktonic foraminiferal δ^{18}O increase at the Eocene/Oligocene boundary recorded the ice volume influence with little temperature effect. Therefore, tropical surface temperatures remained around 22°C while the deep ocean cooled during this δ^{18}O shift.

Following the boundary event, planktonic foraminifera $\delta^{18}O$ record during the Oligocene and early Miocene mirrored the benthic record in many respects. For much of the Oligocene and early Miocene, the absolute values are close to $-0.5‰$, which translates into a temperature estimate of 21°C (**Figure 7B**). By 15 Ma, tropical surface waters had warmed to 26°C.

The middle Miocene $\delta^{18}O$ shift represents an increase of 1.5‰ in the benthic record between 15 and 13 Ma. This transition is composed of two sharp increases around 14 and 13 Ma (**Figure 8B**). These $\delta^{18}O$ steps occurred in less than 200 000 years with each recording an increase of $\sim 1‰$ followed by a small decrease. During these two shifts, deep waters cooled from 9 to 5°C. The planktonic foraminiferal $\delta^{18}O$ record from 15 to 13 Ma shows two increases as recorded in the benthic foraminiferal record (**Figure 7**). However, it does not show the large permanent shift recorded by the benthic foraminifera, indicating a small cooling from 26 to 24°C. From 13 to 3 Ma, the deep ocean cooled slightly from 5 to 3°C while the surface waters warmed from 24 to 26°C (**Figure 7B**).

The last of the large $\delta^{18}O$ steps in the Cenozoic was recorded during the late Pliocene from 3.2 to 2.6 Ma. This 'step' is better characterized as a series of $\delta^{18}O$ cycles with increasing amplitudes and values over this interval (**Figures 6** and **8C**). The cycles have been subsequently determined to be 40 000 year cycles related to variations in the solar radiation received in the high latitudes. This interval ushered in the large-scale Northern Hemisphere ice sheets that have since dominated Earth's climate. At 2.6 Ma, the first IRD was deposited in the open North Atlantic and was coeval with the $\delta^{18}O$ maximum. Prior to 2.6 Ma, IRD was confined to the marginal basins to the north, Greenland's and Iceland's continental margins. Subsequent $\delta^{18}O$ maxima were associated with IRD. Between 2.6 and 1 Ma, large Northern Hemisphere ice sheets waxed and waned on the 40 000 year beat. Beginning around 1 Ma, the ice sheets increased in size and switched to a 100 000 year beat (**Figure 6**). During this interval, deep-water temperatures remained similar to those in the modern ocean (0 to 3°C).

The planktonic foraminiferal $\delta^{18}O$ response during the late Pliocene event shows the cyclic behavior, but not the overall increase recorded by the benthic foraminifera. As with the middle Miocene $\delta^{18}O$ shift, the late Pliocene increase represents the cyclic build-up of ice sheets accompanied by deep water cooling. The tropical surface water temperatures, however, varied between 26 and 28°C.

Mechanisms for Climate Change

Most climate change hypotheses for the Cenozoic focus on either oceanic heat transport and/or greenhouse gas concentrations. Each mechanism produces different responses in the equatorial-to-pole and surface-to-deep temperature gradients. An increase in the meridional heat transport generally cools the tropics and warms the poles. If poleward transport of heat decreases, then the tropics will warm and the poles will cool. Variations in greenhouse gas concentrations should produce similar changes in both the tropical and polar regions.

Tropical surface water and deep-ocean records co-varied for the first part of the Cenozoic. The warming and subsequent cooling between 65 and 34 Ma are most often ascribed to changing greenhouse gas concentrations. The interval of warming that began around 58 Ma and peaked at 52 Ma coincided with the release of large amounts of CO_2 into the atmosphere as a consequence of tectonic processes. The eruption of the Thulean basalts in the north-eastern Atlantic Ocean began during the Paleocene and peaked around 54 Ma. It is also recognized that there was a large-scale reorganization of the midocean ridge hydrothermal system which began during the late Paleocene and extended into the Eocene. Both tectonic processes accelerate mantle degassing which raises atmospheric levels of CO_2. Recently, evidence for another potentially large CO_2 reservoir was found along the eastern continental margin of North America. Methane hydrates frozen within the sediments appear to have released catastrophically at least once and possibly multiple times during the latest Paleocene and early Eocene ($\sim$ 58–52 Ma). One or all of these sources could have contributed to the build-up of greenhouse gases in the atmosphere between 58 and 52 Ma. Following the thermal maximum, the long-term cooling in both the surface and deep waters implies that greenhouse gas concentrations slowly decreased. Proxies for estimating pCO_2 concentrations ($\delta^{13}C$ fractionation within organic carbon and boron isotopes) are still being developed and refined. However, preliminary indications are that atmospheric pCO_2 levels were high (> 1000 p.p.m.) during the early Eocene, dropped to $\sim$ 400–500 p.p.m. during the middle to late Eocene, and reached late Pleistocene concentrations (200–300 p.p.m.) by the early Oligocene.

The deep-water temperature cooling across the Eocene/Oligocene boundary (**Figure 7B**) was not accompanied by tropical cooling, and resulted from the first step in the thermal isolation of Antarctica. In modern ocean, the Antarctic Circumpolar

Current is a vigorous surface-to-bottom current that provides an effective barrier to southward-flowing warm surface waters. The development of this current during the Cenozoic hinged on the deepening for the Tasman Rise and opening of the Drake Passage. Recent drilling indicates that marine connections developed across the Tasman Rise at or near the Eocene/Oligocene boundary (33.5 Ma). Tectonic constraints on the separation of the Drake Passage are less precise. Estimates range from 35 to 22 Ma for the opening of this gateway. The uncertainty lies in the tectonic complexity of the region and what constitutes an effective opening for water to flow through. The climatic consequence of creating a circumpolar flow was to thermally isolate Antarctica and promote the growth of the Antarctic ice sheet. As noted above, the first large ice sheet grew at the beginning at the Eocene/Oligocene boundary.

The most notable divergence in the $\delta^{18}O$ records occurred during the middle Miocene ($\sim$15 Ma). For the first time during the Cenozoic, the tropical surface and deep waters recorded a clear divergence in $\delta^{18}O$ values, a trend that increased in magnitude and reached a maximum in the modern ocean. Any poleward transport of heat appears to have been effectively severed from Antarctica by 15 Ma, promoting further cooling. On the other hand, the tropics have been warming over the past 15 My. A combination of different factors fueled this warming. First, less heat was being transported out of the low- and mid-latitude regions to the high southern latitudes. Second, the opening of the Southern Hemisphere gateways that promoted the formation of the circumpolar circulation led to the destruction of the circumequatorial circulation. The effects of the closure of the Tethys Ocean (predecessor to the Mediterranean), shoaling of the Panamanian Isthmus (4.5–2.6 Ma), and constriction in the Indonesian Passage ($\sim$3 Ma to present) allowed the east-to-west flowing surface waters in the tropics to 'pile' up and absorb more solar radiation. A consequence of the equatorial warming and high-latitude cooling was an increase in the equator-to-pole temperature gradient. As the gradient increased, winds increased, promoting the organization of the surface ocean circulation patterns that persist today.

Some Caveats

A concern in generating marine isotope records is that the isotopic analyses should be made on the same species. This is important because $\delta^{18}O_{calcite}$ values can vary among the different species of organisms. Coexisting taxa of benthic foraminifera record $\delta^{18}O$ values that can differ by as much as 1‰. In planktonic foraminifera, variations between species can be as great as 1.5‰. For both the planktonic and benthic foraminifera, interspecific differences are as large as the glacial–interglacial signal. These interspecific $\delta^{18}O_{calcite}$ variations are often ascribed to a vital effect or kinetic fractionation of the oxygen isotopes within the organism. However, some of the differences in the planktonic taxa results from different seasonal or depth habitats and therefore provides important information about properties in the upper part of the water column. It is noteworthy that the first $\delta^{18}O$ syntheses were based on mixed species analyses and yet basic features captured in these curves still persist today. This attests to the robustness of these records and method for reconstructing climate changes in the ocean.

The high-frequency signal that dominates the late Pliocene to Pleistocene records is also present in the Miocene and Oligocene intervals. The cloud of points about the mean shown in **Figure 7(A)** reflects records that were sampled at a resolution sufficient to document the high frequency signal. For the interval between 35 and 1 Ma, the benthic foraminiferal $\delta^{18}O$ record has a 40 000 year frequency superimposed on the long-term means that are represented by the smoothed line. The origin of the 40 000 year cycles lies in variations in the tilt of the earth's axis that influences the amount of solar radiation received in the high latitudes. This insolation signal is transmitted to the deep ocean because the high latitudes were the source regions for deep waters during much, if not all, of the Cenozoic. The record prior to 35 Ma is unclear with regard to the presence or absence of 40 000 year cycles.

See also

Holocene Climate Variability. Icebergs. Ice-induced Gouging of the Seafloor. Oxygen Isotopes in the Ocean. Sea Ice. Sub Ice-shelf Circulation and Processes.

Further Reading

Craig H (1957) Isotopic standards for carbon and oxygen and correction factors for mass spectrometric analysis of carbon dioxide. *Geochemica et Cosmochemica Acta* 12: 133–149.

Craig H (1965) The measurement of oxygen isotope paleotemperatures. In: Tongiorgi E (ed.) *Stable Isotopes in Oceanographic Studies and Paleotemperatures*, pp. 161–182. Spoleto: Consiglio Nazionale delle Ricerche, Laboratorio di Geologica Nucleare, Pisa.

Craig H and Gordon LI (1965) Deuterium and oxygen-18 variations in the oceans and marine atmosphere. In: Tongiorgi E (ed.) *Stable Isotopes in Oceanographic Studies and Paleotemperatures*, pp. 1–122. Spoleto: Consiglio Nazionale delle Ricerche, Laboratorio di Geologica Nucleare, Pisa.

Emiliani C (1955) Pleistocene temperatures. *Journal of Geology* 63: 539–578.

Epstein S, Buchsbaum R, Lowenstam H and Urey HC (1953) Revised carbonate-water temperature scale. *Bulletin of the Geological Society of America* 64: 1315–1326.

Fairbanks RG, Charles CD and Wright JD (1992) Origin of Melt Water Pulses. In: Taylor RE, Long A and Kra RS (eds) *Radiocarbon After Four Decades*, pp. 473–500. New York: Springer-Verlag.

Imbrie J, Hays JD, Martinson DG *et al.* (1984) The orbital theory of Pleistocene climate: support from a revised chronology of the marine $\delta^{18}O$ record. In: Berger AL, Imbrie J, Hays JD, Kukla G and Saltzman B (eds) *Milankovitch and Climate*, part I, pp. 269–305. Dordrecht: Reidel.

Lear CH, Elderfield H and Wilson PA (1999) Cenozoic deep-sea temperatures and global ice volumes from Mg/Ca in benthic foraminiferal calcite. *Science* 287: 269–272.

Miller KG, Fairbanks RG and Mountain GS (1987) Tertiary oxygen isotope synthesis, sea-level history, and continental margin erosion. *Paleoceanography* 2, 1–19.

Miller KG, Wright JD and Fairbanks RG (1991) Unlocking the Ice House: Oligocene–Miocene oxygen isotopes, eustasy, and margin erosion. *Journal of Geophysical Research* 96: 6829–6848.

Pagani M, Arthur MA and Freeman KH (1999) Miocene evolution of atmospheric carbon dioxide. *Paleoceanography* 14: 273–292.

Palmer MR, Pearson PN and Cobb SJ (1998) Reconstructing past ocean pH-depth profiles. *Science* 282: 1468–1471.

Pearson PN and Palmer MR (1999) Middle Eocene seawater pH and atmospheric carbon dioxide concentrations. *Science* 284: 1824–1826.

Rozanski K, Araguas-Araguas L and Gonfiantini R (1993) Isotopic patterns in modern global precipitation. In: Swart PK, McKenzie J and Savin S (eds) *Climate Change in Continental Isotopic Records*. Geophysical Monograph 78, pp. 1–35. Washington, DC: American Geophysical Union.

Rye DM and Sommer MA (1980) Reconstructing paleotemperature and paleosalinity regimes with oxygen isotopes. In: Rhoads DC and Lutz RA (eds) *Skeletal Growth of Aquatic Organisms*, pp. 162–202. New York: Plenum.

Savin SM, Douglas RG and Stehli FG (1975) Tertiary marine paleotemperatures. *Geological Society of America Bulletin* 86: 1499–1510.

Shackleton NJ (1967) Oxygen isotope analyses and Pleistocene temperatures re-assessed. *Nature* 215: 115–117.

Shackleton NJ, Berger A and Peltier WR (1990) An alternative astronomical calibration of the Lower Pleistocene time scale based on ODP Site 677. *Transactions of the Royal Society of Edinburgh*, *Earth Science* 81: 251–261.

Shackleton NJ and Kennett JP (1975) Paleotemperature history of the Cenozoic and initiation of Antarctic glaciation. Oxygen and carbon isotopic analysis in DSDP Sites 277, 279, and 281. *Initial Report. Deep Sea Drilling Project* 29, 743–755.

Shackleton NJ and Opdyke ND (1973) Oxygen isotope and paleomagnetic stratigraphy of equatorial Pacific core V28-238. Oxygen isotope temperatures and ice volumes on a 10^5 year and 10^6 year scale. *Quaternary Research* 3: 39–55.

Tiedemann RM, Sarnthein M and Shackleton NJ (1994) Astronomic calibration for the Pliocene Atlantic $\delta^{18}O$ and dust flux records of Ocean Drilling Program Site 659. *Paleoceanography* 9: 619–638.

Urey HC (1947) The thermodynamic properties of isotopic substances. *Journal of the Chemical Society* pp. 562–581.

CENOZOIC OCEANS – CARBON CYCLE MODELS

L. François and Y. Goddéris, University of Liège, Liège, Belgium

doi:10.1006/rwos.2001.0253

Introduction

The story of the Cenozoic is essentially a story of global cooling. The last 65 million years of the Earth's history mark the transition from the Cretaceous 'greenhouse' climate toward the present-day 'icehouse' conditions. Particularly, the cooling by about 8–10°C of deep ocean waters since the Cretaceous was linked to a reorganization of the oceanic circulation triggered by tectonic plate movements. These oceanic circulation changes were coeval with continental climatic change, as demonstrated by abundant evidence for global cooling (pollen, faunal assemblages, development of glaciers, etc.). For instance, most of western Europe and the western United States had a subtropical climate during the Eocene, despite the fact that they were located at